

A straight-line wind hit some parts of Bara and Parsa districts of Nepal

Ashok Kumar Pokharel 

Collaborative Innovation Center for Western Ecological Safety, Lanzhou University, Lanzhou, China

This study shows that there was a severe thunderstorm leading to an extreme straight-line wind event in some parts of Bara and Parsa districts of Nepal on 31 March 2019. It occurred due to presence of: (1) an inversion layer above a lower level of deep dry adiabatic layer, (2) moist air at the lower level, (3) a deep dry adiabatic layer above inversion, (4) a veering wind with height, (5) a fairly unidirectional wind from lower mid-levels into upper levels, and (6) wind speed shear at the lower level. As there was no previous history of any analysis of this kind of severe wind system (being of meteorological significance) in Nepal, this study will be quite helpful in improving the understanding of air motion and associated weather and climatic phenomena in Nepal for now and into the future.

Introduction

On 31 March 2019, from about 1300 UTC (1845 local time) onwards, a sudden severe storm hit some parts of Bara and Parsa districts of Nepal¹ and lasted about 30 to 45min in duration, according to local reports. The storm affected areas are about 90km due south from Kathmandu International airport, Nepal (Figures 1 and 2), ranging in altitude from 83 to 109m amsl, and have a hot and humid climate. The extent of the storm damaged area was about 45km long and up to 33km wide (i.e. the distance between the parallel lines of storm affected locations). But due to the lack of radiosonde and radar data, as well as skilled/trained weather forecasters in the country, it was not forecast before it hit. In total, the storm killed 28 people, injured hundreds and destroyed a huge amount of public property.² To investigate this event, this study attempts to fill the gap of under-

¹<https://www.unicef.org/nepal/stories/bara-and-parsa-storm>

²<https://myrepublica.nagariknetwork.com/news/10-latest-developments-on-bara-parsa-tragedy-with-photos/>

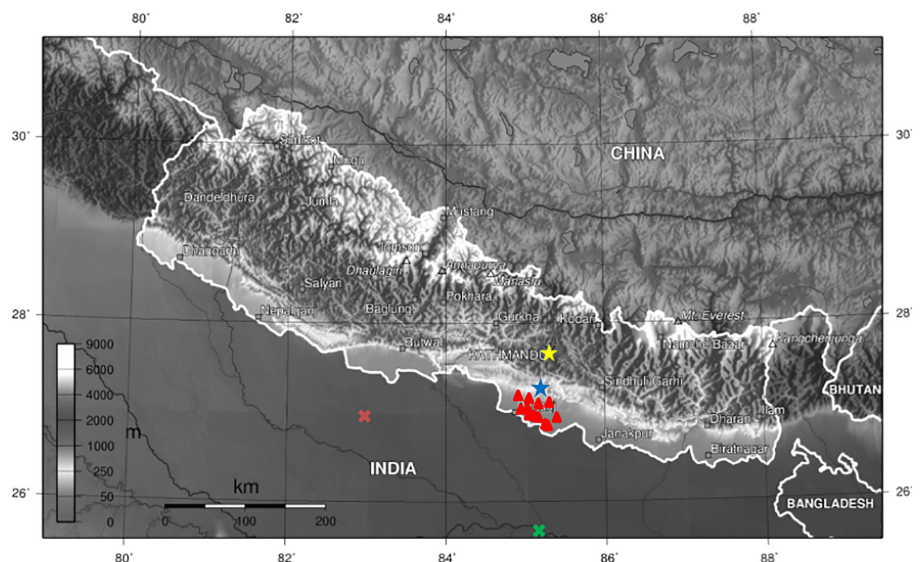


Figure 1. Red coloured triangles indicate the storm affected locations (Jaganathpur, Bhaluhi, Parwanipur, Prasauni, Pheta, Purainiya, Dharamnagar, Rampurwa, Dharmnagar, Mahagadhimai, Devtaal, Hardiya, Benauli, Bairiya, Parchrouwa and Gamariya) of Bara and Parsa districts of Nepal on 31 March 2019. The blue and yellow stars indicate Simara (domestic) and Kathmandu airports (international) in Nepal, respectively, and green and red crosses indicate atmospheric sounding stations at Patna and Gorakhpur in India, respectively. (Source: https://www.researchgate.net/figure/Topographical-map-of-Nepal_fig1_230779096.)



Figure 2. Destruction of homes in Purainiya village of Parsa district of Nepal caused by the storm on 31 March 2019. (Source: <https://myrepublica.nagariknetwork.com/news/10-latest-developments-on-bara-parsa-tragedy-with-photos/>.)

standing of atmospheric processes responsible for causing this storm, and hopefully for similar type of events in the future. Here, it

is hypothesised that these very strong gusts of wind were due to a severe thunderstorm with extreme straight-line winds.

Data and methods

Satellite images from Moderate Resolution Imaging Spectroradiometer (MODIS)/Terra (EOSDIS Worldview, 2019) were collected and analysed. Reanalysis data sets of geopotential height, wind speed and direction were obtained from the second Modern Era Retrospective-Analysis for Research and Application ($0.50^{\circ} \times 0.67^{\circ}$) (MERRA-2, 1980; Rienecker *et al.*, 2011), in order to make horizontal cross sections for the synoptic scale observational analysis. Rawinsonde data were obtained from the University of Wyoming, USA,

which were also analysed. With the help of 0.5° resolution data sets obtained from National Oceanic and Atmospheric Administration / Global Forecast System (NOAA/GFS), modelled atmospheric soundings were also generated and analysed in depth. Surface weather station plots, containing data such as surface pressure, wind speed/direction and air temperature, in and around the storm area on that particular day, were also collected from the Department of Hydrology and Meteorology, Nepal (DHM, Nepal). Similarly, field photographs taken after the event were gathered from different sources, and were also analysed.

Results and discussion

A visible satellite image captured by MODIS/Terra shows a shelf cloud (i.e. a horizontal and wedge-shaped cloud, which covered the entire horizon, and is formed on the leading edge of the gust front of a thunderstorm) over the storm affected area on that particular storm day (Figure 3). Surface weather plots obtained from the DHM, Nepal, show that a surface low pressure system had formed prior to the event in and around the storm affected area, as shown in Figures 4(a) and (b). To determine the vertical temperature and wind speed/direction profiles at different pressure levels close to the affected area, the soundings at 0000 UTC (local time 0530 in India and 0545 in Nepal) on 31 March 2019 at Patna (25.6°N 85.1°E , elevation 60m amsl) and Gorakhpur (26.75°N 83.36°E , elevation 77m amsl) were consulted (Figures 5a and b). As Patna and Gorakhpur lie 174km south and 161km west, respectively, from the storm affected area, it was expected that an analysis of the vertical profiles of different meteorological variables from Patna and Gorakhpur, before and after the event, could be fruitful.

Figures 5(a) and (b) show that in the lowest level of the planetary boundary layer (PBL) there was an inversion below a deep dry adiabatic layer. Based on the magnitudes of convective available potential energy (CAPE) (1658 and 2201Jkg^{-1} at Patna and Gorakhpur stations, respectively), lifted index (LI) values (-4.72 and -7.12 at Patna and Gorakhpur stations, respectively), an inversion at lower levels early in the day (0000 UTC on 31 March 2019), the veering of wind and directional wind speed shear

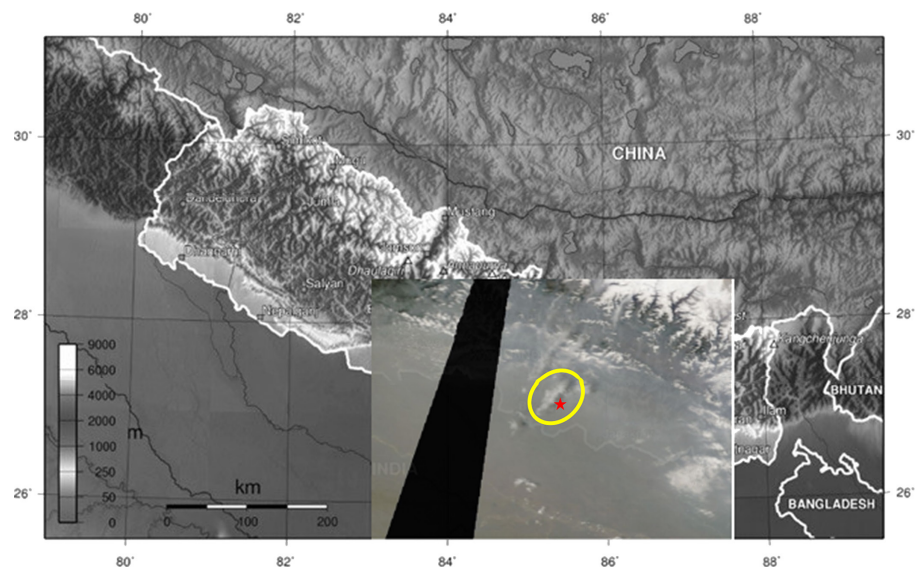


Figure 3. A visible satellite image captured by MODIS/Terra over storm affected area on 31 March 2019. This satellite image is superimposed on the political map to recognise the area marked by yellow circle where storm took place. Yellow circled area shows the shelf cloud (i.e. white elongated cloud) over the storm affected area. A red coloured star shows one of the storm affected locations (called Pheta) of Bara district where the windstorm hit severely.

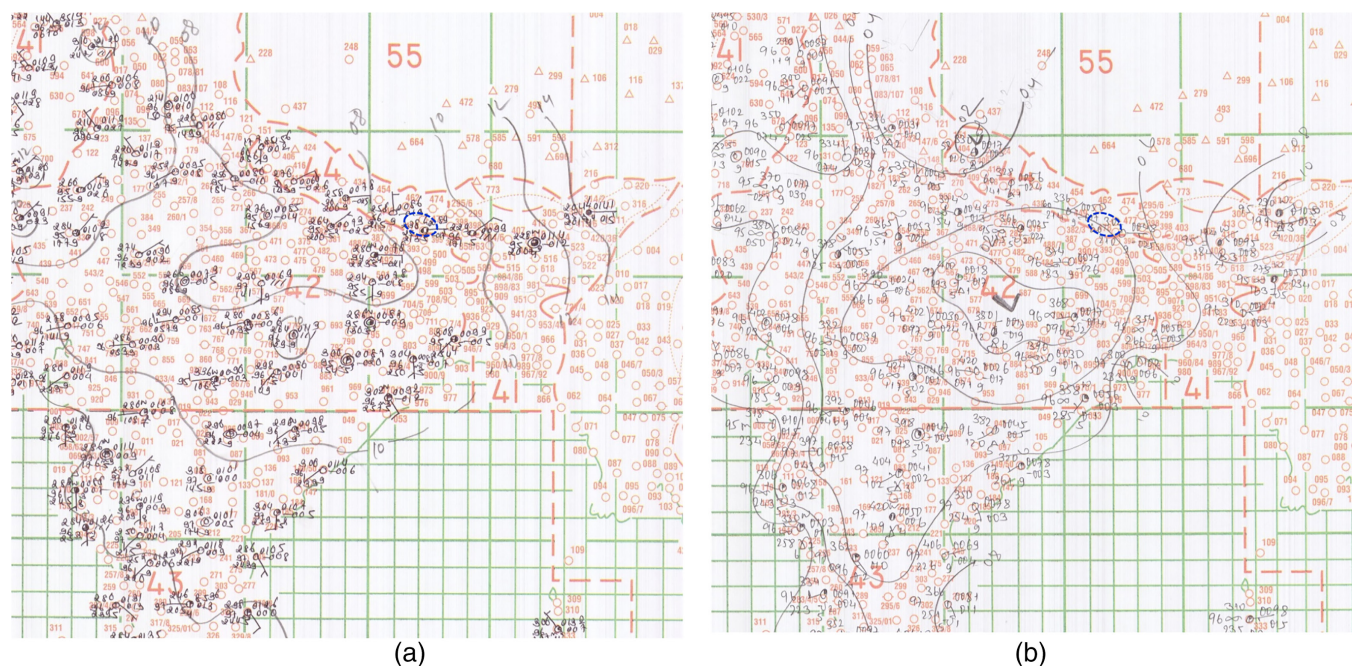


Figure 4. (a) A surface weather map plot in and around the storm affected area at 0300 UTC on 31 March 2019. (b) Same, but for 0900 UTC on 31 March 2019. The blue circle indicates the storm affected area. (Source: Department of Hydrology and Meteorology, Nepal (DHM, Nepal).)

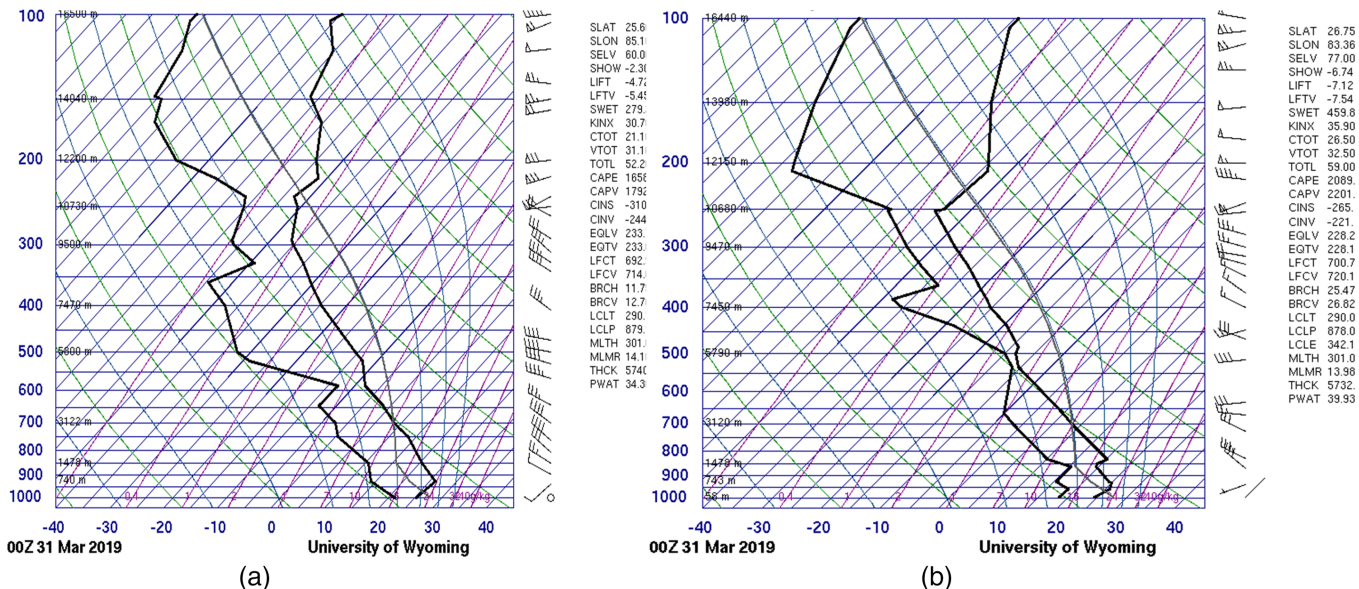


Figure 5. (a) Atmospheric soundings observed at 0000 UTC at Patna, India on 31 March 2019. (b) Atmospheric sounding observed at 0000 UTC at Gorakhpur, India on 31 March 2019. (Source: University of Wyoming, USA.)

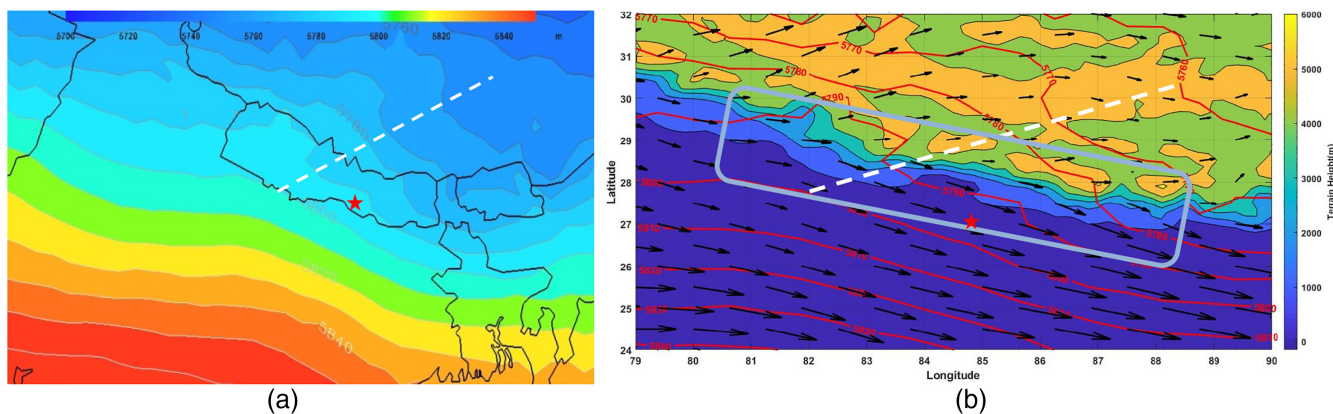


Figure 6. (a) Geopotential height, in steps of 10m, showing synoptic overview of the system at 0630 UTC (1215 local time) on 31 March 2019, using MERRA-2 data. The white dotted line indicates a trough axis oriented northeast-southwest. The dark red to dark blue height contours depict the highest to the lowest pressure, respectively. (b) Geopotential height, in steps of 10m, showing a synoptic overview of the system at 0630 UTC (1215 local time) on 31 March 2019, using MERRA-2 data. The white dotted line indicates the trough axis oriented northeast-southwest. The black arrows show the wind field (please note that bold and long black arrows indicate the strong wind field called the jet streak). The blue rectangle indicates the geographical location (latitude/longitude) of Nepal. The red star in both plots, shows one of the storm affected locations (called Pheta) of Bara district of Nepal where the windstorm hit severely.

at lower levels, a high dew point (21°C and 18°C at Patna and Gorakhpur stations, respectively) and an air temperature of 25°C at low levels for each of these two stations, as well as the deep dry adiabatic lapse rates above the inversion observed in the two soundings, it can be stated that there was a significant chance of a thunderstorm in and around the stations during the afternoon. It is to be noted here that CAPE defines the amount of energy available for a developing thunderstorm. It infers the instability of the atmosphere, and also provides an approximation of updraft strength within a thunderstorm. Similarly, the LI is a stability index which helps to determine the buoyancy of the atmosphere, and is computed using the temperature difference between the environment and an air parcel lifted adiabatically at a given pressure height in the mid-troposphere of the atmosphere.

Before and during this particular event, the mid-tropospheric synoptic overview was also analysed using MERRA-2 data sets. The 500hPa geopotential height, wind speed and direction at 0630 UTC (1215 local time in Nepal) show that before the occurrence of the storm there was a positively tilted trough over the region of interest (Figure 6a). Similarly, a jet streak was also moving from the northwest to the southeast at 500hPa. Over time (1230 UTC) the jet was continuously advancing, influencing the trough and the baroclinic amplification of the jet streak was consistent with the deepening of the trough at that time (Figure 6b). It is to be noted here that upper level trough and the jet streak were the main ingredients for the formation of the thunderstorm as the presence of upper level trough generated strong positive vorticity advection and created differential tempera-

ture advection, whilst the presence of jet streak favoured the lifting of air parcels.

Time-wise soundings are also plotted here as a tool to understand the stability of the atmosphere, to see weather elements at every layer in the atmosphere, and to determine additional characteristics of this particular event (Figures 7a-d). Using NOAA/GFS data sets several modelled atmospheric soundings for Simara Airport in Nepal (27.16°N, 84.98°E, elevation 137m amsl), which is located approximately 8.75km from the storm affected area, were plotted and analysed at different time intervals for 31 March 2019 (Figures 1 and 7a-c). Figure 7(a) shows that there was an inversion layer at the 950–925hPa level, and a deep dry adiabatic layer lay above 925hPa at 0000 UTC (0545 local time) on 31 March 2019. This is consistent with Patna and Gorakhpur soundings as mentioned earlier

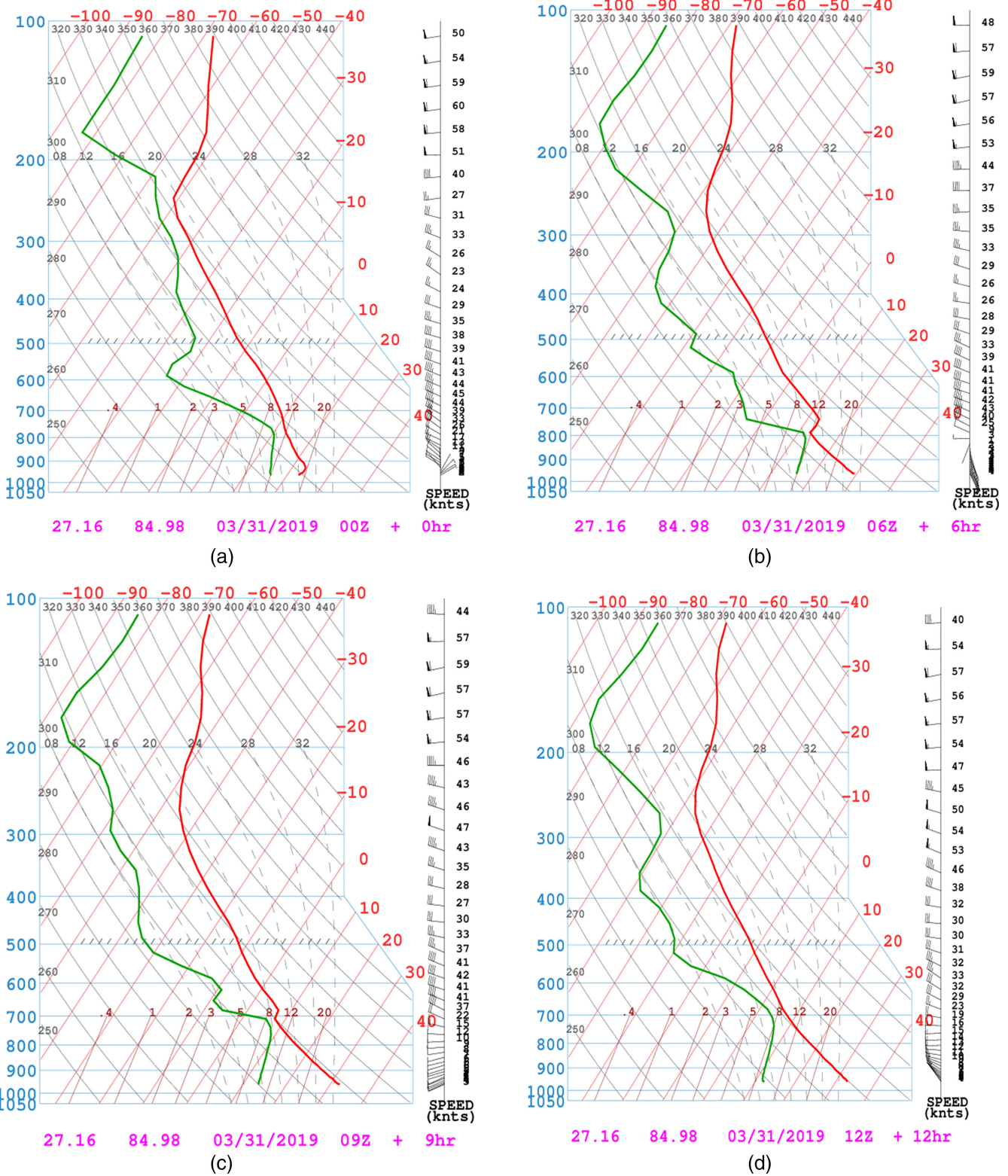


Figure 7. (a) Modelled atmospheric sounding plotted for Simara airport, Nepal at 0000 UTC (0545 local time) on 31 March 2019 using NOAA/GFS data sets of 0.5° resolution. (b) Same for 0600 UTC (1145 local time) on 31 March 2019. (c) Same for 0900 UTC (1445 local time) on 31 March 2019. (d) Same for 1200 UTC (1745 local time) on 31 March 2019. Red and green lines indicate temperature and the dewpoint, respectively.

(Figures 5a and b). The soundings at 0600 to 0900 UTC (1145 to 1445 local time) have an inverted “V”-shape, indicating the following conditions at that time: (1) The surface dew point and surface air temperature were about 13–15°C and 32°C, respectively; (2) an inversion lay above the lower level deep dry adiabatic layer; (3) the presence of moist air at the lower level; (4) a deep dry adiabatic

layer (i.e. dry air) above the near-surface inversion; (5) the presence of veering wind with height; (6) the wind direction remained fairly unidirectional from lower mid-levels into upper levels; and (7) wind speed shear was present at lower levels (Figures 7b and c). This reveals that as the day advanced, there was presence of moisture, instability, lift and directional wind shear and strong

wind speeds. Specifically, these data sets infer that wind had a veering directional change of 60° or more from the surface to 700hPa; the upper level wind speed was greater than 70kn (36.01ms⁻¹); and the 850 to 700hPa wind (i.e. low level jet) was 25kn (12.86ms⁻¹) or greater, besides the presence of the strong upper level trough and the jet as discussed earlier.



Figure 8. Field photographs after the event on 31 March 2019. (a) Red colour arrows, which are parallel to each other, show the push of the debris (green leaves) in the direction of wind. (Source: <https://myrepublica.nagariknetwork.com/news/photo-feature-storm-kills-28-400-injured/?categoryId=81>). (b) Showing the push of the debris (crops and the fallen trees) in the direction of wind. (Source: <https://kathmandupost.com/money/2019/04/05/gone-with-the-wind-crops-worth-millions-destroyed-in-rainstorm>.)

These time-wise soundings also reveal that dewpoint depression decreased significantly with height, with dry air in the lower troposphere and nearly saturated air in the middle troposphere, with the presence of inversion separating the dry air aloft and the moist air near the surface, and the convective condensation level (CCL) at a high elevation (more than 1300m). All of these were ingredients for the occurrence of a severe thunderstorm. Therefore, based on these data sets, the different processes responsible for generating a strong wind from a severe thunderstorm are thus described below.

Initially a capping inversion existed from the surface to a certain height, with heat, moisture and instability building under this 'cap' into the afternoon (Figures 7b and c). Over time (1200 UTC - local time 1745), the cap broke due to daytime sensible heating and the existence of all of the additional ingredients as discussed earlier. The outcome was explosive convection, resulting in severe wind gusts (Figure 7d). This was due to the entrainment of dry air aloft into the downdrafts. This promoted evaporative cooling and further enhanced the negative buoyancy of air parcels. In this way, a cold parcel of air surrounded by warm air descended faster than the surrounding air since the cold air is denser, and cooler air is often noticed at the surface when a downburst reaches the surface.

All of the aforesaid data sets indicate that there was a severe thunderstorm leading to a severe straight-line wind event. This wind was produced by the downward momentum in the downdraft region of a thunderstorm. An environment conducive to a strong straight-line wind is one in which both the updrafts and thus downdrafts were strong, the air was dry in the middle troposphere, and the storm had a fast forward motion. It is also to be noted that severe straight-line

winds occur in association with an inverted "V" sounding, i.e. the dewpoint depression decreases significantly with height. This is consistent with the shape of 0600 and 0900 UTC soundings (Figures 7b and c). The sounding at 1200 UTC (Figure 7d) indicates that there was a break of the inversion layer and release of strong winds, which is also supported by a statement of the DHM, Nepal, when they estimated strong winds of more than 90kmh/56mph (more than 25.03ms^{-1}) at that time.³ It is to be noted here that if winds meet or exceed 25.9ms^{-1} then the storm is classified as severe thunderstorm by the National Weather Service (NWS), USA. Besides this, a satellite image (Figure 3) and the field photos show that there was a shelf cloud that produced a severe straight-line wind event, resulting from a severe thunderstorm⁴ over the affected area, and the orientation of the resulting debris was in the direction of the wind (Figures 8a and b). It is important to note that when the NWS, USA, does a storm damage survey after a severe storm, they first distinguish different storms based on the nature of the damage in and around the track of the storm⁴. For example, they define a straight-line wind effect if there is a path of debris in the direction of the wind (and which is consistent with the field photographs, Figures 8a and b).^{5,6}

³https://www.facebook.com/actionaid.nep/posts/2311060008953163?comment_id=2313415488717615

⁴<https://whnt.com/weather/valleywx-blog/straight-line-winds-or-a-tornado-what-caused-saturdays-storm-damage/>

⁵<https://myrepublica.nagariknetwork.com/news/photo-feature-storm-kills-28-400-injured/?categoryId=81>

⁶<https://kathmandupost.com/money/2019/04/05/gone-with-the-wind-crops-worth-millions-destroyed-in-rainstorm>

To sum up, the reanalysis and soundings data sets, surface plots, the satellite image and the field photographs clearly indicate that there was an occurrence of straight-line wind generated from the severe thunderstorm.

Conclusion

Until now, there have been no previous published documents severe of straight-line wind storms in Nepal. This study is therefore of benefit in helping to define this kind of severe event in the future. It also emphasises the necessity for the establishment of a weather radar, the launching of routine atmospheric soundings system over this region, the upgrading of the existing weather forecasting system, and the building of capacity of weather forecasters in Nepal so that there will be a more reliable and efficient forecasting system in the future, which will help save people's lives and their property for days to come.

Acknowledgements

I would like to thank Second Tibetan Plateau Scientific Expedition and Research Program (STEP), grant no. 2019QZKK0602, the National Natural Science Foundation of China under grants 41991231, and 41975075, and the China 111 Project (no. B13045) for providing financial support for this publication. I would also like to thank the Department of Hydrology and Meteorology, Nepal (DHM, Nepal) for providing surface weather data sets. Thanks to the Editor, Dr Edward Graham, and two anonymous reviewers whose constructive comments and suggestions greatly improved the overall quality of this paper.

References

EOSDIS Worldview. 2019. The satellite imagery. <https://worldview.earthdata.nasa.gov> [accessed 5 April 2021].

MERRA-2. 1980. *The second modern-era retrospective analysis for research and applications*. https://disc.sci.gsfc.nasa.gov/mdisc/data-holdings/merra/merra_products_nonjs.shtml [accessed 9 April 2021].

Rinecker MM, Suarez MJ, Gelaro R et al. 2011. MERRA: NASA's modern-era retrospective analysis for research and applications. *J. Clim.* **24**: 3624–2648.

Correspondence to: A. K. Pokharel
ashokpokharel@hotmail.com

© 2021 The Author. Weather published by John Wiley & Sons Ltd on behalf of the Royal Meteorological Society

This is an open access article under the terms of the Creative Commons Attribution-NonCommercial-NoDerivs License, which permits use and distribution in any medium, provided the original work is properly cited, the use is non-commercial and no modifications or adaptations are made.

doi: 10.1002/wea.4050